Signal transduction of insulin

Diabetes mellitus is a severe chronic disease, affecting 6-11 percent of the populations aged 30-64 and about 20 percent of those older than age 65 throughout the world. Diabetes is reaching pandemic proportions, largely owing to an increase in type II diabetes, as the lifespan is extended and more agricultural and subsistence economies adopt "westernized" lifestyles. The purpose of the seminar is to review the insulin receptor-mediated signal transduction process and discuss some experimental data related to the pathogenesis of type II diabetes mellitus.

History

Although there may be older references in Chinese literature to a fatal wasting disease with increased urination, the first description of diabetes appears in the Ebers papyrus in 1500 BC. The term "diabetes", coined by Demetrios of Apamaia in 200 BC, is derived from the Greek word diabeinein, meaning siphon. It was meant to capture the excessive urination and "melting down of flesh and limb into urine". The Latin appellation "mellitus", meaning honey, was added centuries later with the recognition that the urine of diabetics was sweet tasting. The clear distinction between diabetes mellitus and another endocrine disease associated with voluminous urination, diabetes insipidus, was made in the 18th century. The modern era, characterized by experimentation, followed. Sugar was identified in 1838 as the substance conferring the sweet taste to diabetic urine. Subsequent investigations revealed the role of the liver and pancreas, and of the pancreatic islet cells in particular, in the development of diabetes. The preparation of an active pancreatic extract and its usage for treatments of dogs, and then humans by Frederick Banting, Charles Best, JJR Macleod, and JB Collip followed. Until the first successful insulin treatment in a 14-year-old boy in 1922, the acute onset of diabetes during childhood was a death sentence. If children did not die with the initial episode of diabetic coma, they almost all perished in the next 1-2 years. With insulin therapy, the "juvenile-onset" type of diabetes was no longer acutely fatal. With longer survival, however, a variety of long-term complications appeared including blindness, renal failure, loss of legs, myocardial infarction or stroke. Diabetes had been transformed from the disease which was "short, disgusting and painful" , as described by Arateus in the 1st century, into a chronic condition that was long, disgusting, and more painful. Although much of the interest of early physicians and investigators was focused on the "juvenile-onset" form of diabetes, it is only part of the story. In the late 19th century, another form of diabetes was described by Lacereaux, which occurred later in life, mostly in the well- do, and responded to a change in the diet. He named this form "fat diabetes", to distinguish it from the fatal, "thin diabetes" in children and young people. In the mid 1930s, Himsworth proposed the terms "insulin-sensitive" and "insulin-resistant" to designate the two different clinical presentations of diabetes. During the last decades of the 20th century, an enormous amount of data has been accumulated, which led to therapies achieving an improved control of blood glucose levels, and thus, delaying the onset of devastating long-term complications. Diabetes mellitus is now recognized as a syndrome, and comprises a heterogeneous collection of disorders, with type II diabetes, by far the most common presentation.

Clinical diabetes

Definition-Diabetes mellitus is a heterogenous set of disorders characterized by two features: disordered metabolism, most notably hyperglycemia, and the propensity to develop specific long-term complications, such as retinopathy, nephropathy, macro-, and microangiopathy, and neuropathy. The underlying cause of all forms of diabetes is relative or absolute insulin deficiency.

Classification-**Type I** (formerly "insulin-dependent" or "juvenile-onset") diabetes mellitus is caused by pancreatic β-cell destruction, often autoimune-mediated, that leads to loss of insulin secretion and absolute insulin deficiency. Comprises 5-10% of all cases in the diabetes syndrome. **Type II** (formerly "noninsulin-dependent" or "adult-onset") diabetes mellitus is caused by combination of genetic and nongenetic factors that result in insulin resistance and relative insulin deficiency, insufficient to meet increased demands imposed by insulin resistance. The specific genes are not

known, but are under intensive investigation. Nongenetic factors include increasing age, high-calorie intake, overweight, central adiposity, sedentary lifestyle, and low birth-weight. Comprises 90-95% of all cases. **Other specific types** of diabetes include a heterogeneous group of cases with genetic defects in insulin secretion or insulin action, as well as a large number of well-defined illnesses leading to secondary disturbances in insulin resistance, insulin secretion, or both. Only 1-2 % of all diabetes mellitus cases belong to this group. **Gestational diabetes** is defined as diabetes with onset during pregnancy. Occurs in 3-5% of all pregnancies. Usually remits after delivery, but returns later as type II diabetes in about 50% of women who had gestational diabetes.

A brief natural history of type II diabetes mellitus-The majority of type II diabetes occurs after age 40, with more than 50 % of the cases after age 55. The disease, however, has an insidious onset, and often goes undetected because the symptoms are either unrecognized or ignored. Type II diabetes results from the interaction of genetic and environmental factors. There is an almost 100 % concordance in identical twins, it runs through families (having one type II diabetic parent means a 2-fold risk, having two diabetic parents means a 4-fold risk to develop the disease), its prevalence in ethnically diverse communities varies by the genetic background, and is extremly common in certain inbred populations. Although a genetic background for the susceptibility to type II diabetes is widely recognized, the specific genes have yet to be identified. The development of the disease is strongly influenced by environmental factors, while 50 % of Pima Indians living in a reservation in Arizona present with type II diabetes, Pima Indians in Mexico, farming and living at a subsistence level, have not developed diabetes. Similarly, the prevalence in Nauru is 40%, but the native Nauruan population did not develop diabetes until the mining of guano changed their lifestyle from subsistence fishing and farming to a sedentary lifestyle, with motorbikes, high-fat diet and obesity. Obesity, and the central (or abdominal) obesity form in particular, is also associated with type II diabetes, but usually only a small proportion of obese people contract the disease.

Development of type II diabetes. Insulin resistance, simply expressed as reduced sensitivity to the effects of insulin, is the most common underlying abnormality in type II diabetes, and it is detectable in people way before the onset of symptoms. The state seems to be fueled by obesity. β-Cells of the pancreas normally compensate for insulin resistance by increasing basal and postprandial insulin secretion. At some point, β-cells can no longer compensate, failing to respond appropriately to glucose. This leads to the development of glucose intolerance, and in a year 5-10% of the patients with glucose tolerance progress to diabetes mellitus, which continues to worsen as insulin resistance increases. In the late stages of the disease β-cells undergo complete failure and high doses of exogenous insulin may be required.

Insulin receptor-mediated signal transduction

Insulin receptor

The insulin receptor is a transmembrane glycoprotein, composed of two α subunits and two β subunits covalently linked through disulfide bridges to form an α2β2 heterotetramer. The α subunit is entirely extracellular and contains the sites for insulin binding, the β subunit has a small extracellular portion, a transmembrane domain and an intracellular portion having insulin-regulated protein tyrosine kinase activity. In the absence of insulin, the α subunit suppresses the tyrosin kinase activity of the β subunit. Binding of insulin to the α subunit results in a conformational change that releases inhibitory constraints and allows tyrosine kinase activity. The receptor then undergoes a series of intramolecular transphosphorylations in which one β subunit phosphorylates tyrosine residues in the adjacent β subunit. This autophosphorylation regulates the tyrosine kinase activity of the C-terminal part and precedes the tyrosine phosphorylation of endogeneous substrates. In addition to tyrosine phosphorylation,

the insulin receptor may undergo serine and threonine phosphorylation, e.g. by cAMP-dependent protein kinase, or protein kinase C. In contrast to tyrosine phosphorylation, serine phosphorylation has a negative effect on receptor tyrosine kinase activity. Serine phosphorylation has been suggested to play a role in the decreased receptor tyrosine kinase activity observed in type II diabetes, but exact details and relationships remain unclear. Counterregulatory hormons, like epinephrine may antagonize insulin action by serine phosphorylation of the receptor.
Naturally occurring mutations of the insulin receptor are rare, and the phenotype, when present, shows severe insulin resistance. Some of these mutations are classified as "other types" of diabetes mellitus, but according to genomic analysis mutations in the insulin receptor do not play a role in the development of typical type II diabetes mellitus.

Phosphorylation targets of the insulin-activated receptor tyrosine kinase
Once activated, the insulin receptor phosphorylates a number of substrates, including members of the insulin receptor substrate family (IRS-1, IRS-2, IRS-3, IRS-4). IRS proteins recognize and bind to phosphorylated tyrosine residues in the insulin receptor and once phosphorylated by the receptor tyrosine kinase, will serve as docking proteins for signaling molecules that have SH2 (Src-homology) domains, such as PI3K (phosphatidylinositol 3 kinase), SHP2 (a tyrosine phosphatase), and Grb2 (a small adaptor molecule). The tissue distribution of the various isoforms is different, while IRS-1 and IRS-2 are ubiquitously expressed, IRS-3 is mainly restricted to the adipose tissue, and IRS-4 is most abundant in kidney and brain.
Genetic polymorphisms influencing the IRS family have been described, and although none by itself is associated with the disease, certain combinations of the polymorphisms are more frequent in type II diabetics than in the normal population.

Molecular events downstream from the IRS proteins
Divergence of the insulin-signaling pathway into metabolic, growth promoting, and other biological effects probably occurs at the level of SH2 adaptor proteins that bind to phosphorylated tyrosine residues through their SH2 domains. Grb-2 is an SH2 adaptor protein that docks with IRS upon insulin stimulation and initiates processes leading to the activation of the MAP kinase cascade. This cascade mediates the mitogenic effects of insulin, and is commonly activated by other growth factor receptors than insulin.
The key element of the pathway leading to the metabolic effects of insulin is probably the activation of phosphatidylinositol 3 kinase (PI3K). PI3K is a heterodimer consisting of a regulatory subunit (p85) that associates with IRS and a catalytic subunit (p110) that phosphorylates phosphatidylinositols in the cellular membrane at position 3 in the inositol ring. Phosphatidylinositol 3,4,5-trisphosphate activates PDK1 (PI3K-dependent kinase 1) and the downstream sequence of events includes activation of protein kinase B (also named Akt), isoforms of protein kinase C (ξ,γ), mTOR (mammalian target of rapamycin) and P70S6 kinase. Protein kinase B is a Ser/Thr kinase with substrates including glycogen synthase kinase-3 (GSK-3), cAMP response element binding protein, and certain transcription factors. mTOR is a member of the PI3K family, and its substrates are Ser residues in proteins. mTOR increases translation via the p70S6 kinase. Collectively, these kinase cascades mediate the metabolic effects of insulin, such as translocation of GLUT4 transporters from intracellular pools to the plasma membrane, stimulation of glycogen and protein

synthesis, and initiation of specific gene transcription (e.g. glucokinase). There is also a PI3K-independent pathway that mediates insulin-stimulated glucose transport.

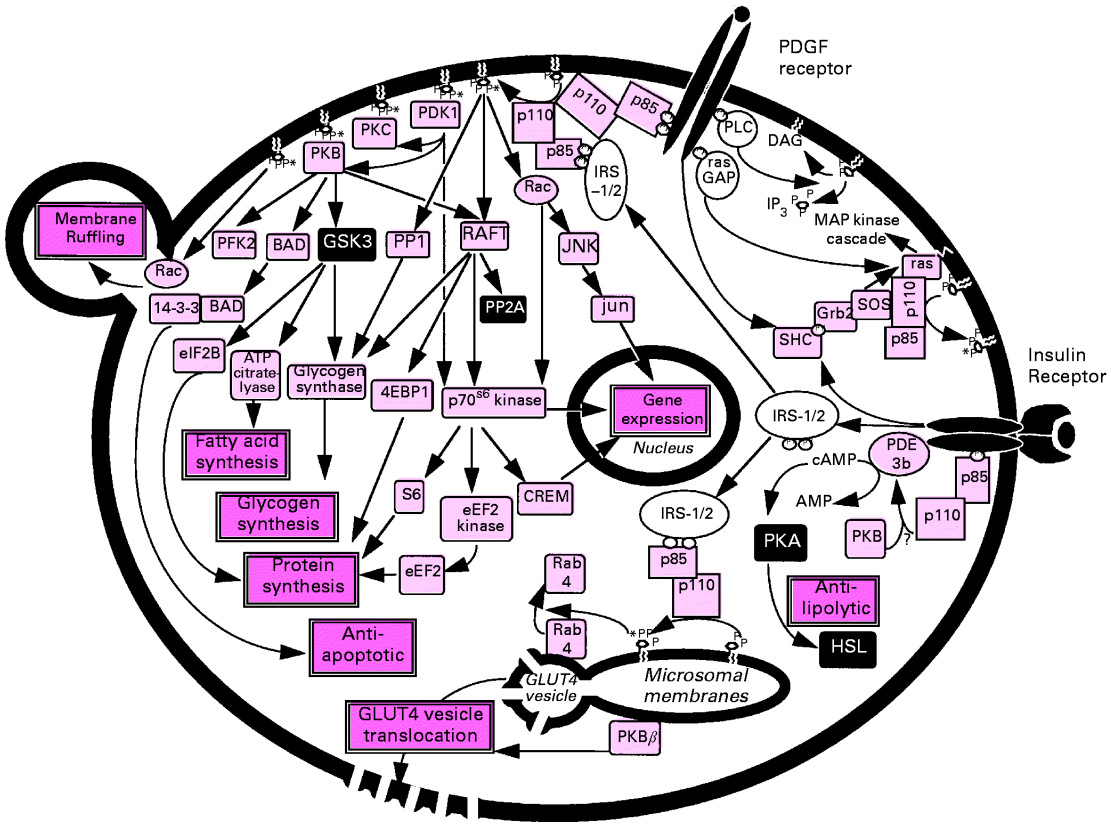

Figure. Summary of insulin-mediated signal transduction

β-Cell dysfunction in type II diabetes mellitus

Regulation of blood glucose level requires that pancreatic β-cells adapt their insulin secretion to the fluctuations in blood glucose concentration. Glucose equilibrates across the plasma membrane and is phosphorylated to glucose-6-phosphate by glucokinase. In b-cells this step determines the rate of glycolysis and the rate of pyruvate formation. Thus, when blood glucose level is high, the rate of glycolysis in the β-cells will increase. Compared to other cell types, an unusually high portion of pyruvate will enter the mitochondria and the citric acid cycle ensuring a significant rise in mitochondrial ATP production, and the ATP is exported to the cytosol. The increase in the ATP:ADP ratio in the cytosol causes depolarization of the plasma membrane by the closure of ATP-sensitive K^+ channels. This allows the opening of voltage-sensitive Ca^{2+} channels, and the increase in cytosolic Ca^{2+} concentration triggers the exocytosis of insulin-containing secretory granules.

Some rare forms of DM are attributed to genetic defects that impair the adequate insulin response by interfering with the signaling pathways in β-cells (e.g. glucokinase, or transcription factors).

In type II DM no genetic abnormalities profoundly effect β-cell function, but rather the ability of β-cells to adapt to insulin resistance that occur over lifetime. In high proportion of subjects with insulin resistance, β-cell compensation maintains normal glucose tolerance and DM may never develop. The compensatory hypersecretion of

insulin in insulin-resistant states is due to an expansion of β-cell mass and alterations in the expression of key enzymes of β-cell glucose metabolism. The factors that determine the ability of the β-cell to compensate for insulin resistance are unknown. Although several mutations have been described that increase the risk of developing type II DM via impairing β-cell function, there is no clear understanding of the molecular background resulting in the manifestation of the disease.

Topics for discussion

1, Metabolic processes regulated by insulin that play a major role in the regulation of blood sugar level: a, stimulation of glucose transport in muscle and adipose tissue, b, increased rates of glucose utilization in tissues, as a consequence of decreased rate of utilization of fatty acids, c, decreased rate of glucose output from the liver

2, To appreciate the role of the IRS proteins in insulin-mediated signal transduction and the development of diabetes, discuss the following experiments:

Araki E, et al. Alternative pathway of insulin signalling in mice with targeted disruption of the IRS-1 gene. Nature 1994, 372:186-190, Figs 2-4.

Is there a relationship between the IRS-1 gene and growth rate? Are IRS-1 knock out mice resistant to insulin? Does the absence of IRS-1 influence the phosphorylation of the insulin receptor or PI3K? What could be the reason for the IRS-1 knock out mice do not present with diabetes?

Withers DJ, et al. Disruption of IRS-2 causes type 2 diabetes in mice. Nature 1998, 391:900-904, Figs 1e, 2-4.

Background information: insulin resistance is quantitatively characterized using the euglycemic hyperinsulinemic clamp method: the amount of glucose required for maintainance of the same blood glucose level is measured in the course of insulin infusion. Since hepatic glucose output influences the amount of glucose required, hepatic glucose output is determined by an independent method, and used for calculation of glucose disposal rate in the euglycemic hyperinsulinemic clamp method.

Note the similarities between the last Figure and the clinical experience: IRS-1 knock out mice present with insulin resistance, but β-cell compensation prevents the development of diabetes. In IRS-2 knock out mice, however, insulin resistance occurs with β-cell deficiency leading to a diabetic phenotype.

Compare the following data described in IRS-1 KO mice and IRS-2 KO mice: growth rate, glucose metabolism, PI3K phosphorylation, and pancreas islet cell morphology.

Liu SCH, et al. Insulin receptor substrate 3 is not essential for growth or glucose homeostasis. J Biol Chem 1999, 274:18093-18099, Figs 2-6, Table 1.

Using similar methods, no alteration has been found in IRS-3 KO mice in terms of growth rate and glucose metabolism.

3, Role of protein kinase B in the insulin-mediated inactivation of glycogen synthase kinase-3:

Cross DAE, et al. Inhibition of glycogen synthase kinase-3 by insulin mediated by protein kinase B. Nature 1995, 378:785-789, Figs 1, 2, 3a.

Background information: Glycogen synthase is active when dephosphorylated, and can be inactivated by Ser-phosphorylation. Insulin inhibits the cAMP-dependent protein kinase, and the glycogen

synthase kinase-3 (GSK-3), and activates the phosphoprotein phosphatase-1 pool located at the glycogen particles in a PI3K-dependent way.

Is the insulin-induced GSK-3 inactivation related to the MAP kinase cascade or to the PI3K pathway? What is the role of protein kinase B?

4, The molecular link between obesity and insulin resistance is not well defined, but several potential mechanisms have been recently described (see review paper below) As an example, discuss the following paper:

Uysal KT, et al. Protection from obesity-induced insulin resistance in mice lacking TNF-α function. Nature 1997, 389:610-614.

What kind of models were utilized to demonstrate the relationship between obesity and insulin resistance? What is the effect of TNF-α deficiency?

Review papers:
Saltiel AR, and Kahn CR. Insulin signalling and the regulation of glucose and lipid metabolism. Nature 2001, 414:799-806.

Shepherd PR, Withers DJ, and Siddle K. Phosphoinositide 3-kinase: the key switch mechanism in insulin signalling. Biochem J 1998, 333:471-490.

Zick Y. Insulin resistance: a phosphorylation-based uncoupling of insulin signaling. Trends in Cell Biol 2001, 11:437-441.

Selected figures

Araki E, et al. Alternative pathway of insulin signalling in mice with targeted disruption of the IRS-1 gene. Nature 1994, 372:186-190, Figs 1f, 2-4.

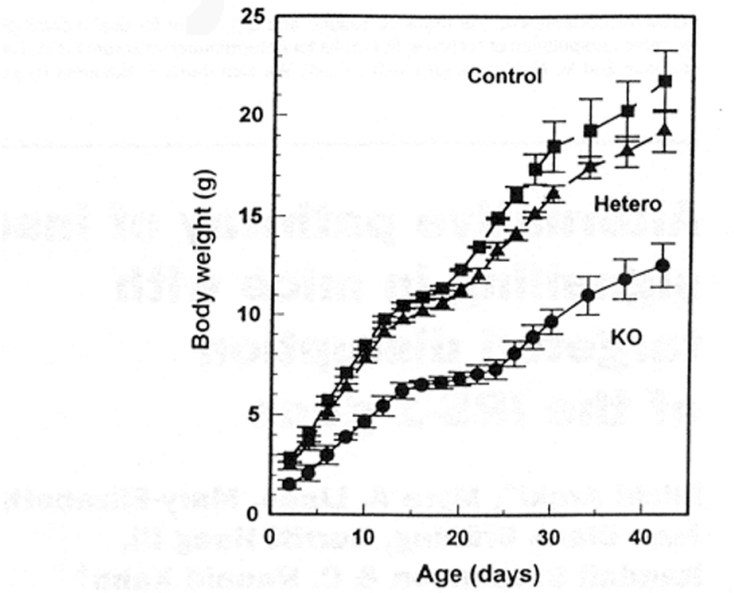

Figure 1f. Growth curves of IRS-1 $^{+}/^{+}$ (control), heterozygous (Hetero) and homozygous IRS-1$^{-}/^{-}$ mutant (knock out, KO) mice. Data are from two litters and are representative of 60 animals. Values are mean ±SEM of three IRS-1 $^{+}/^{+}$, four IRS-1 $^{+}/^{-}$, and four IRS-1 $^{-}/^{-}$ animals.

FIG. 2 Blood glucose and plasma insulin (*a*), glucose tolerance tests (*b*), insulin/IGF-1 tolerance tests (*c* and *d*) and glucose uptake in adipocytes (*e*) in *IRS-1*$^{-/-}$ and *IRS-1*$^{+/+}$ mice.
METHODS. Blood glucose concentrations and plasma insulin levels (*a*) were measured between 8:00 and 10:00 a.m. after overnight fasting on 4–8-week old anaesthetized mice. Immunoreactive insulin concentrations in plasma were measured by radioimmunoassay. Insulin (*c*) and IGF-1 (*d*) tolerance tests were performed after a 6-hour fast on 6–16-week-old mice using an intraperitoneal injection of either 0.75 IU per kg human insulin or 1 mg per kg IGF-1 (Eli Lilly). Results are expressed as a percentage change from fasting blood glucose concentration and were not significantly different between groups. Glucose tolerance tests (*b*) were done on IRS-1-deficient and wild-type animals after a fasting for 6 h by intraperitoneal injection of 2 g D-glucose per kg at time zero. Data were obtained from at least 8 animals in each group, ranging in age from 5–12 weeks. Results are mean ± s.e.m. Asterisks in *a*–*d*: *, $P<0.05$; **, $P<0.025$; and ***, $P<0.01$. Glucose transport was measured in isolated adipocytes (*e*). After a 4-hour fast, male mice (12–20 weeks old) were anaesthetized by intraperitoneal injection of 115 mg kg^{-1} sodium pentobarbital (Abbott Laboratories). As soon as pedal and corneal reflexes stopped, the epididymal fat pads were removed. Adipocytes were isolated by digesting epididymal fat pads for 1 h in Krebs–Ringer HEPES (30 mM) buffer containing 1 mg ml^{-1} collagenase (Worthington), 200 nM adenosine and 2.5% BSA (Sigma) as described[30]. Cells (~10^5 ml^{-1}) were incubated for 30 min in the absence or presence of human insulin. Glucose transport was then assayed for a further 30 min using 3 μM universal ^{14}C-glucose (286 mCi mmol^{-1}; Amersham). The reaction was stopped by spinning cells for 30 s through 100 μl dinonyl phthalate. Microfuge tubes were cut through the oil layer, and the upper phase containing the cell layer was counted for incorporated radioactivity. Data are mean ± s.e.m. of four mice in each group in four independent experiments with triplicate determinations. **, $P<0.025$.

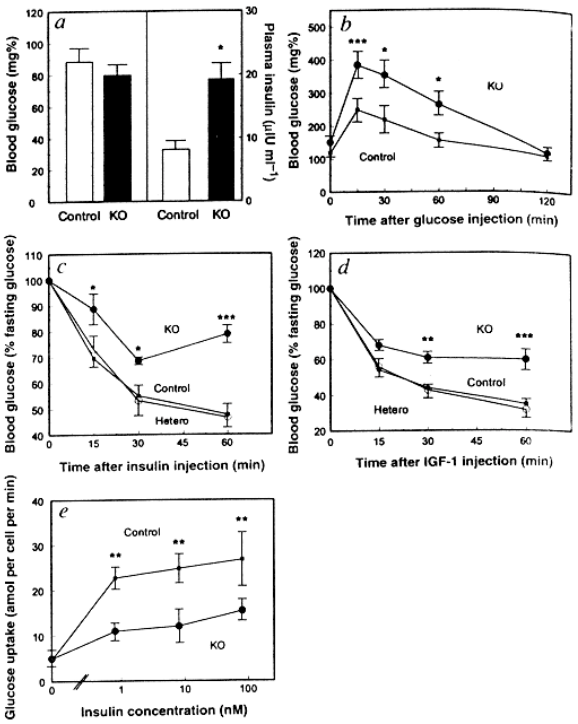

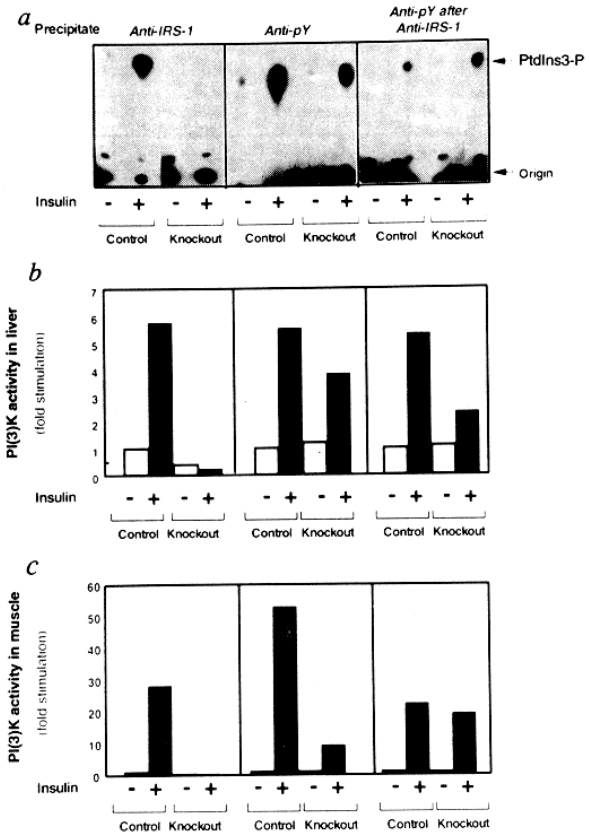

FIG. 3 Insulin-stimulated activation of PI(3)K in the *IRS-1*$^{-/-}$ mouse. Supernatants of liver or muscle homogenates containing equal amounts of protein were immunoprecipitated in duplicate with the indicated antibody; immunoprecipitates were washed extensively and assayed *in vitro* for PI(3)K activity. *a*, Representative panel from an experiment using liver homogenates. *b*, Liver PI(3)K activity was assayed in supernatants of liver homogenates containing 5–10 mg total protein after immunoprecipitation with the indicated antibody. *c*, Muscle PI(3)K activity was measured in supernatants of homogenates containing 2.5–5 mg total protein following immunoprecipitation with the indicated antibody. For *b* and *c*, data are the mean of three separate experiments in seven *IRS-1*$^{-/-}$ and six *IRS-1*$^{+/+}$ mice and are expressed as fold stimulation of activity above that of the non-insulin-treated controls.
METHODS. Five units of regular human insulin (Lilly) were injected as a bolus into the inferior vena cava of anesthetized mice. The liver, gastrocnemius and quadriceps muscles were removed at 1, 2.5 and 3 min after insulin injection, respectively, and homogenized at 4 °C as described[11]. Liver and muscle homogenates were allowed to solubilize at 4 °C for 1 h and clarified by centrifugation at 15,000 r.p.m. for 1 h. Supernatants containing equal amounts of protein were immunoprecipitated overnight with anti-IRS-1 C-terminal (6 μg ml^{-1}), antiphosphotyrosine 4G10 (3 μg ml^{-1}) (from M. White), anti-insulin receptor C-terminal (3 μg ml^{-1}) or control rabbit serum. Immune complexes were collected with 120 μl of a 50% slurry of protein A–Sepharose (Pharmacia). Supernatants of samples that were initially precipitated with anti-IRS-1 antibody were reprecipitated with anti-phosphotyrosine antibody in a similar manner. All immunoprecipitates were washed extensively. The PI(3)K reaction was performed as described[11]. ^{32}P incorporation into phosphatidylinositol-3-phosphate (PtdIns-3-P) was quantified using a Phosphorimager (Molecular Dynamics).

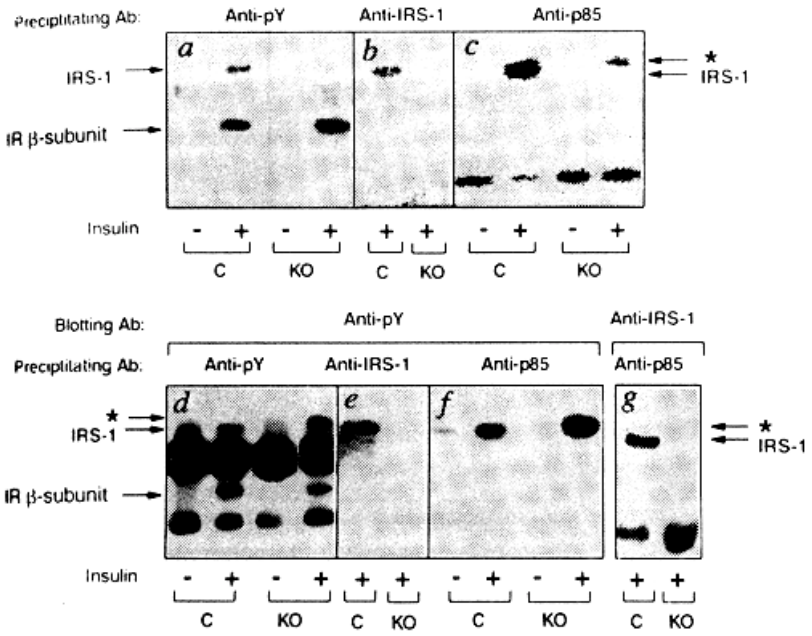

FIG. 4 Phosphotyrosine proteins in muscle and liver or *IRS-1*$^{-/-}$ mice. *a–c*, Muscle homogenate (3.5 mg) from insulin-treated or control mice were immunoprecipitated with the indicated antibodies and subjected to reducing SDS–PAGE and western blotting with anti-phosphotyrosine antibodies. The migration of the tyrosine-phosphorylated protein (IRS-2) detected in anti-phosphotyrosine and anti-p85 immunoprecipitates from the IRS-1-knockout animal following insulin stimulation is indicated by the asterisk and is about 10K above that of IRS-1. Each lane represents tissue from one animal; each blot is representative of at least 3 experiments. *d–g*, Liver homogenate (9 mg) from insulin-treated or control mice was immunoprecipitated with the indicated antibodies and subjected to reducing SDS–PAGE and western blotting with anti-phosphotyrosine antibodies (*d*, *e*, *f*) or anti-IRS-1 antibody (*g*). Each lane represents tissue from one animal; each blot is representative of at least 3 experiments.

METHODS. Frozen liver and muscle samples previously collected at 1.5 and 3.5 min, respectively, after insulin injection were powdered and immediately homogenized in buffer containing 50 mM HEPES (pH 7.4), 50 mM sodium pyrophosphate, 100 mM sodium fluoride, 10 mM EDTA, 10 mM sodium orthovanadate, 1% Triton X-100, 10 μg ml^{-1} aprotinin, 5 μg ml^{-1} leupeptin, 2 mM benzamidine and 2 mM PMSF. Homogenates were allowed to solubilize for 1 h at 4 °C before centrifugation at 55,000 r.p.m. for 1 h. Supernatants containing equal amounts of total liver or muscle protein were immunoprecipitated overnight with the indicated antibody. Immune complexes were collected with protein A–Sepharose, washed, solubilized in Laemmli sample buffer and separated using 6% SDS–PAGE. Proteins were transferred to nitrocellulose, probed with anti-phosphotyrosine or anti-IRS-1 C-terminal antibodies, detected with ^{125}I-labelled protein A, and visualized by autoradiography. Polyclonal antibodies to mouse p85 α-subunit of PI(3)K and the monoclonal antiphosphotyrosine antibody 4G10 were from M. White.

Withers DJ, et al. Disruption of IRS-2 causes type 2 diabetes in mice. Nature 1998, 391:900-904, Figs 1e, 2-4.

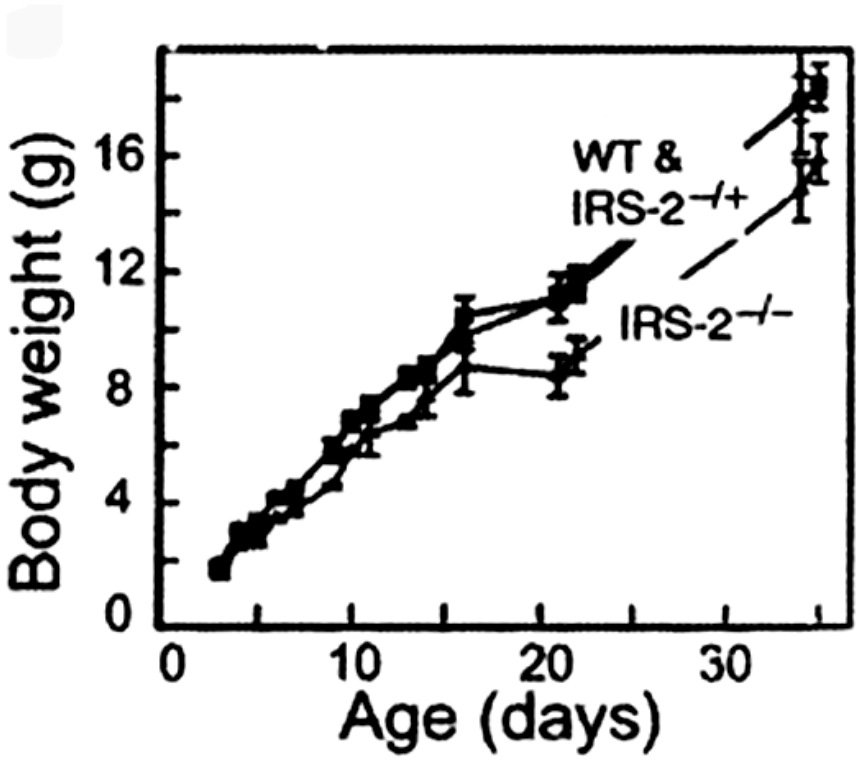

Figure 1f. Growth curves of wild type (WT), heterozygous (IRS-2 $^{+/-}$) and homozygous IRS-2$^{-/-}$ mutant (IRS-2$^{-/-}$) mice. Data are from six litters with a total of at least 15 animals per genotype. Representative of 60 animals. Values are mean ±SEM.

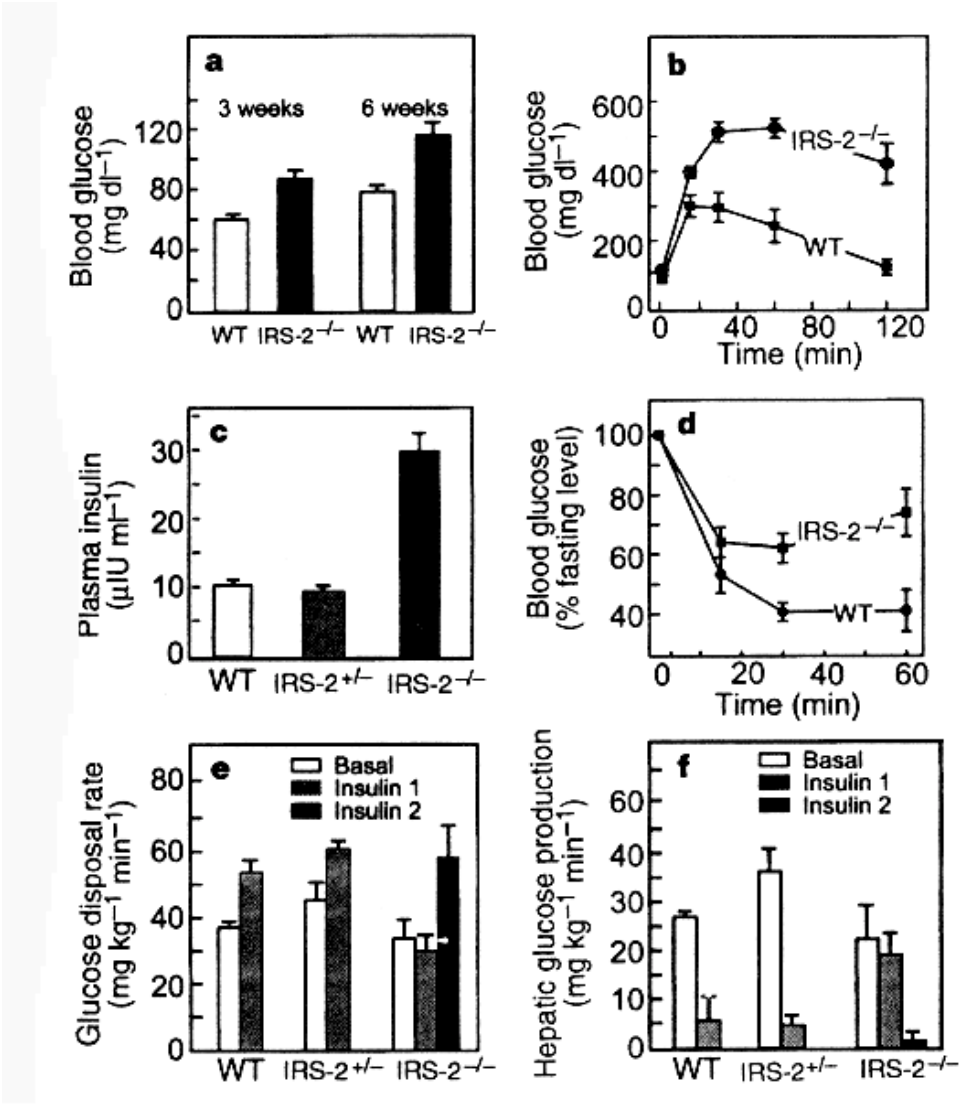

Figure 2 Fasting blood glucose and glucose-tolerance test, fasting insulin levels and insulin-tolerance test, and *in vivo* glucose disposal and hepatic glucose production. **a**, After a 15 h overnight fast, blood glucose levels were determined using a Glucometer Elite glucometer (Bayer). Results are mean values ± s.e.m. for at least eight animals per genotype, with ages as indicated. WT, wild type. **b**, Glucose-tolerance tests after intraperitoneal loading with 2 g D-glucose per kg were performed on 6-week-old animals of the indicated genotype. Results are mean values ± s.e.m. for at least eight animals per genotype. **c**, Serum insulin levels were measured by radioimmunoassay on 4–6-week-old anaesthetized animals after a 15 h overnight fast. Data are the mean values ± s.e.m. for at least 12 animals per genotype. **d**, Insulin-tolerance tests were performed on fed 4–6-week-old animals. Results are expressed as percentage of initial blood glucose concentration and are the mean values ± s.e.m. for at least eight animals per genotype. **e**, Glucose-disposal rate and **f** hepatic glucose production rate were determined on fasted, conscious 8-week-old mice using the euglycaemic hyperinsulinaemic clamp. Basal rates and those stimulated by infusion of insulin at a rate of 2.5 mU kg^{-1} min^{-1} (insulin 1) and 20 mU kg^{-1} min^{-1} (insulin 2) were determined. Results are the mean values ± s.e.m. for three animals per genotype.

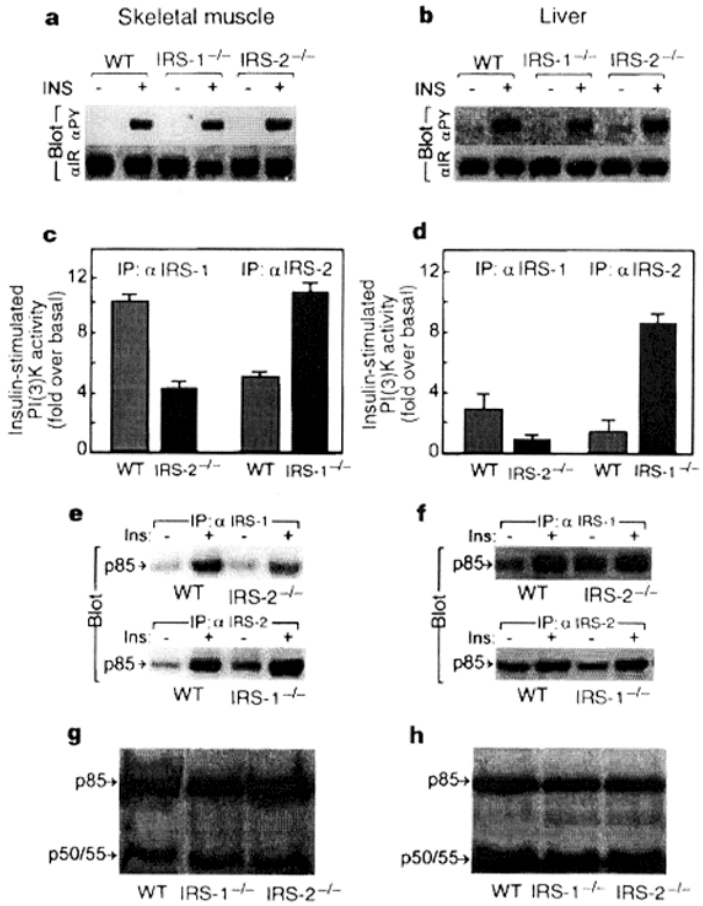

Figure 3 Expression and insulin-stimulated tyrosine phosphorylation of the insulin receptor (IR), insulin-stimulated activation of PI(3)K and IRS association with p85, and expression of PI(3)K adaptor subunits in the liver and muscle of wild-type (WT), *IRS-1*$^{-/-}$ and *IRS-2*$^{-/-}$ mice. Supernatants of muscle (**a**) or liver (**b**) homogenates containing equal amounts of protein from untreated and insulin (INS)-treated 4–6-week-old mice were immunoprecipitated with anti-IRβ antibody and blotted for either antiphosphotyrosine (αPY) or IRβ (αIR). Data are representative of data obtained from three animals per genotype. Supernatants of muscle (**c**) or liver (**d**) homogenates containing equal amounts of protein from untreated and insulin-treated 4–6-week-old mice were immunoprecipitated (IP) in duplicate with the indicated antibody (αIRS-1 or αIRS-2); immunoprecipitates were assayed *in vitro* for PI(3)K activity. Data are the mean values ± s.e.m. of two independent experiments and represent data from a total of eight wild-type, nine *IRS-2*$^{-/-}$ and four *IRS-1*$^{-/-}$ animals. Results are expressed as fold stimulation of activity above that of non-insulin-treated controls (fold stimulation over basal). Muscle (**e**) and liver (**f**) homogenates treated as above were immunoprecipitated with the indicated antibody (αIRS-1 or αIRS-2) and subjected to western analysis to study association with p85α/β. Data are representative of data obtained from three animals per genotype. Ins, insulin. Muscle (**g**) and liver (**h** lysates from animals of the indicated genotypes were subjected to SDS-PAGE and western blotting with an anti-p85 SH2 domain antiserum, which recognize p85α/β and the p50/55 splice variants. Data are representative of those obtained from three animals per genotype.

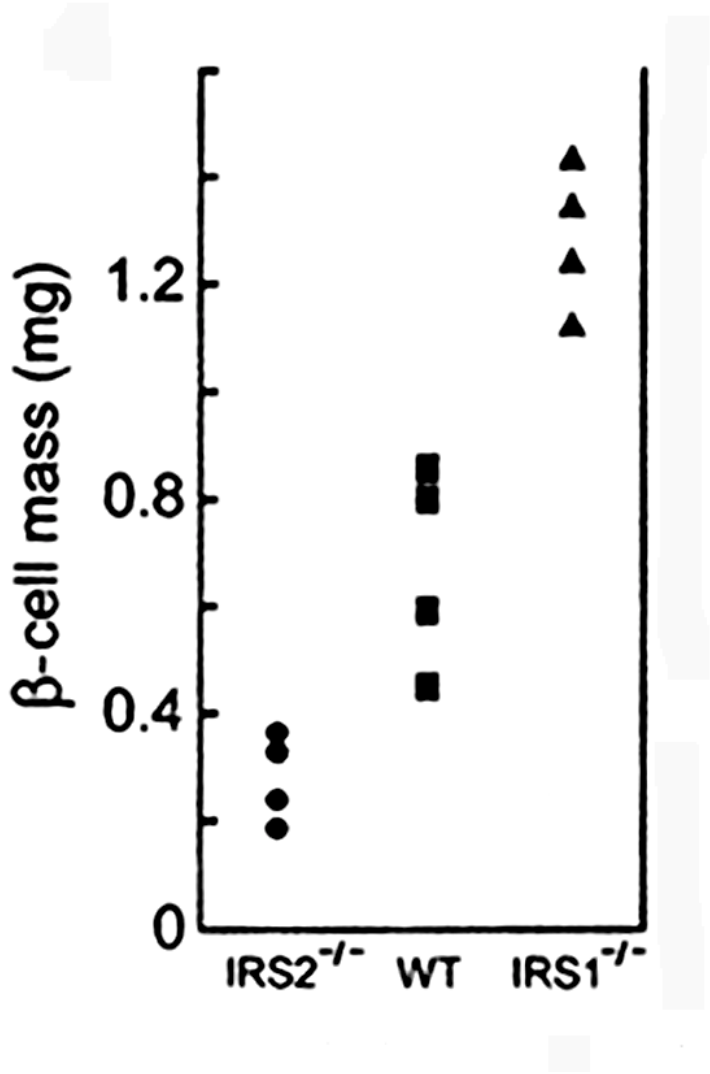

Figure 4. Quantification of β-cell mass by point-counting morphometric analysis on sections from the same mice analyzed blind for the genotype. Mean total pancreatic weights (g) ± SEM for each genotype were : wild type (WT) 178 ± 19, IRS-2 $^{-/-}$ 123 ± 12, and IRS-1 $^{-/-}$ 113 ± 9 (n=4).

Cross DAE, et al. Inhibition of glycogen synthase kinase-3 by insulin mediated by protein kinase B. Nature 1995, 378:785-789, Figs 1, 2, 3a.

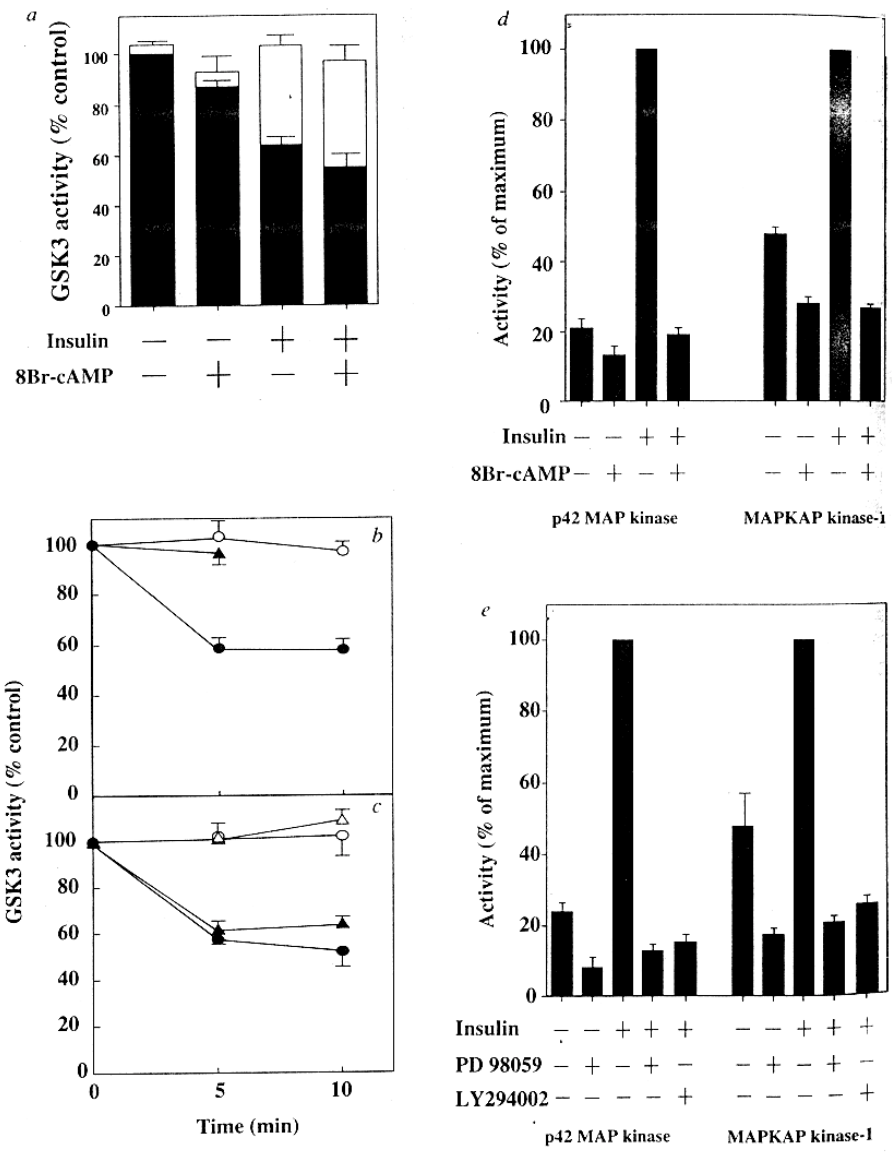

FIG. 1 The inhibition of GSK3 by insulin in L6 myotubes is unaffected by agents that prevent activation of the classical MAP kinase pathway. All the results (±s.e.m.) are for at least three experiments. *a*, L6 myotubes were incubated for 15 min with 2 mM 8-bromocyclic-AMP (8Br-cAMP) and then with 0.1 μM insulin (5 min). Both GSK3 isoforms were co-immunoprecipitated from the lysates and assayed before (black bars) and after (white bars) reactivation with $PP2A_1$[10]. The results are presented relative to the activity in unstimulated cells, which was 0.08 ± 0.006 U mg^{-1} ($n = 10$). *b*, *c*, The inhibition of GSK3 by insulin (0.1 μM) is unaffected by rapamycin (0.1 μM) and PD 98059 (50 μM), but prevented by LY 294002 (100 μM). *b*, L6 myotubes were stimulated with insulin for the times indicated with (filled triangle) or without (filled circles) a 15-min preincubation with LY 294002, and GSK3 measured as in *a*. The open circles show experiments from insulin-stimulated cells where GSK3 was assayed after reactivation with $PP2A_1$[10]. In *c*, cells were incubated with rapamycin (triangles) or rapamycin plus PD 98059 (circles) before stimulation with insulin, and GSK3 activity measured as in *a*, before (filled symbols) and after (open symbols) pretreatment with PP2A. *d*, *e*, L6 myotubes were incubated with 8Br-cAMP (15 min), PD 98059 (60 min) or LY 294002 (15 min) and then with insulin (5 min) as in *a*–*c*. Each enzyme was assayed after immunoprecipitation from lysates, and the results are presented relative to the activities obtained in the presence of insulin and absence of 8Br-cAMP, which were 0.04 ± 0.005 U mg^{-1} (p42 MAP kinase, $n = 6$) and 0.071 ± 0.004 U mg^{-1} (MAPKAP kinase-1, $n = 6$). METHODS. Monolayers of L6 cells were cultured until myotubes had formed, stimulated and lysed as described previously[10]. p42 MAP kinase, MAPKAP kinase 1 or (GSK3-α plus GSK3-β) were then immunoprecipitated from the lysates and assayed with specific protein or peptide substrates as described previously[10]. One unit of protein kinase activity was that amount which catalysed the phosphorylation of 1 nmol of substrate in 1 min. Where indicated, GSK3 in immunoprecipitates was reactivated with $PP2A_1$[10].

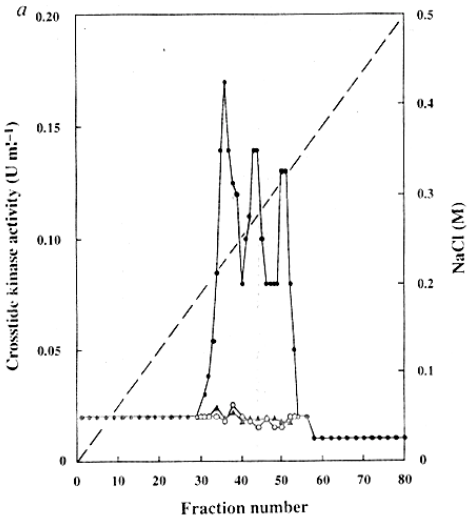

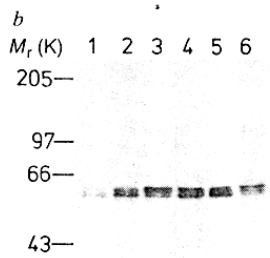

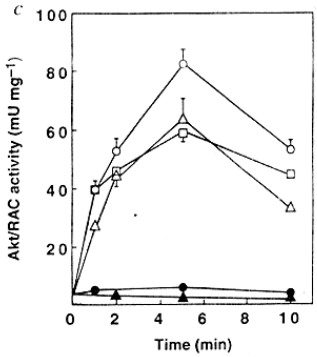

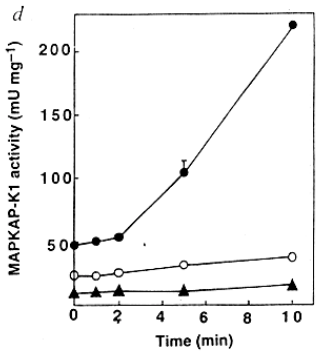

FIG. 2 Identification of PKB as the insulin-stimulated, wortmannin-sensitive and PD 98059/rapamycin-insensitive Crosstide kinase in L6 myotubes. *a*, Cells were incubated with 50 μM PD 98059 (for 1 h) and 0.1 μM rapamycin (10 min), then stimulated with 0.1 μM insulin (5 min) and lysed[10]. The lysates (0.3 mg protein) were chromatographed on Mono Q (5 × 0.16 cm) and fractions (0.05 ml) were assayed for Crosstide kinase (filled circles). In separate experiments insulin was omitted (open circles) or wortmannin (0.1 μM) added 10 min before the insulin (filled triangles). The broken line shows the NaCl gradient. Similar results were obtained in six experiments. *b*, Pooled fractions (10 μl) 31–34 (lane 1), 35–38 (lane 2), 39–42 (lane 3), 43–45 (lane 4), 46–49 (lane 5) and 50–53 (lane 6) from *a* were electrophoresed on a 10% SDS/polyacrylamide gel and immunoblotted with the C-terminal anti-PKB-α antibody. Marker proteins are indicated. No immunoreactive species were present in fractions 1–30 or 54–80. *c*, L6 myotubes were stimulated with 0.1 μM insulin and PKB immunoprecipitated from the lysates (50 μg protein) essentially as described previously[10], using the anti-PH domain antibody and assayed for Crosstide kinase (open circles). In control experiments, myotubes were incubated with 0.1 μM rapamycin plus 50 μM PD 98059 (open triangles) or 2 mM 8Br-cAMP (open squares), or 0.1 μM wortmannin (filled circles) or 100 μM LY 294002 (filled triangles) before stimulation with insulin. *d*, As *c*, except that MAPKAP kinase-1 was immunoprecipitated from the lysates and assayed with S6 peptide (filled circles). In control experiments, cells were incubated with 0.1 μM rapamycin plus 50 μM PD 98059 (filled triangles) or with 2 mM 8Br-cAMP (open circles) before stimulation with insulin. In *c* and *d*, the error bars denote triplicate determinations, and similar results were obtained in three separate experiments.

METHODS. Mono Q chromatography was performed as described[13], except that the buffer also contained 1 mM EGTA, 0.1 mM sodium orthovanadate and 0.5% (w/v) Triton X-100. Two anti-PKB-α antibodies were raised in rabbits against the C-terminal peptide FPQFSYSASSTA and bacterially expressed PH domain of PKB-α. The C-terminal antibody was affinity purified[21]. The activity of PKB towards Crosstide is threefold higher than its activity towards histone H2B and 11-fold higher than its activity towards myelin basic protein, the substrates used previously to assay PKB. Other experimental details and units of protein kinase activity are given in Fig. 1.

Figure 3a. GSK-3 is inactivated by PKB from insulin-stimulated L6 myotubes. Cells were stimulated for 5 min with 0.1 μM insulin, and PKB immunoprecipitated from 100 μg of cell lysate and used to inactivate GSK-3 isoforms. Black bars show GSK-3 activity measured after incubation with PKB as a percentage of the activity obtained in control incubations where PKB was omitted. In the absence of PKB, GSK-3 activity was stable throughout the experiment. The white bars show the activity after reactivation of GSK-3 with $PP2A_1$. No inactivation of GSK-3 occurred if insulin was omitted, or if wortmannin (0.1μM) was added 10 min before the insulin or if the anti-PKB antibody was incubated with peptide immunogen (0.5 mM) before immunoprecipitation. The results (± SEM) are for three experiments (each carried out in triplicate).

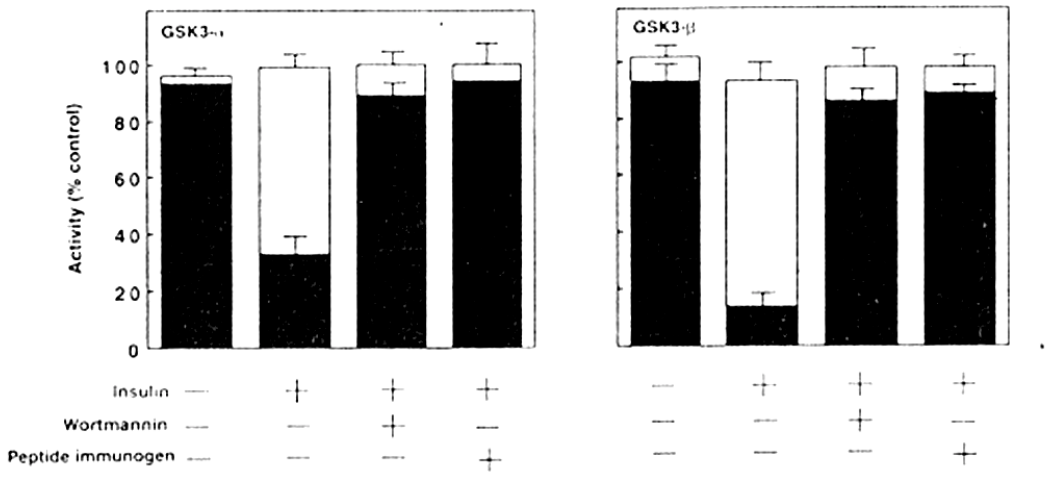

Uysal KT, et al. Protection from obesity-induced insulin resistance in mice lacking TNF-α function. Nature 1997, 389:610-614.

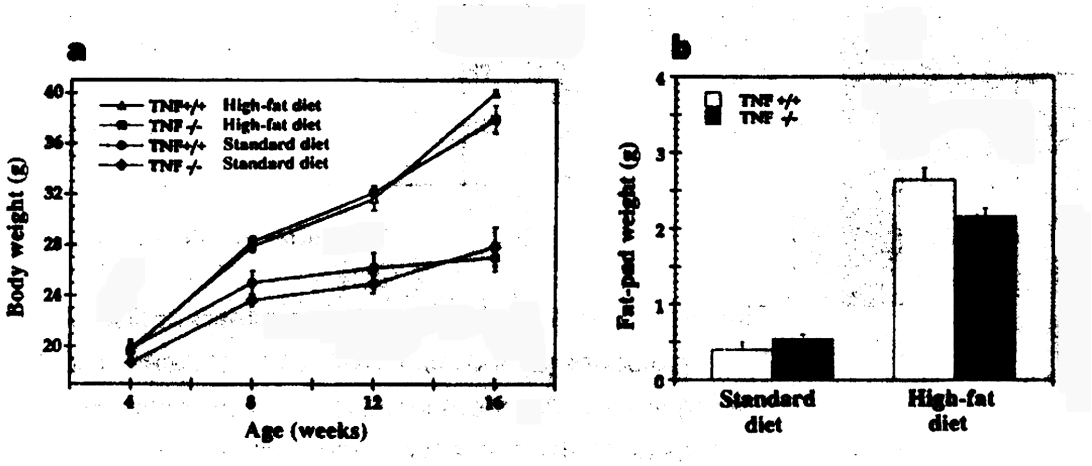

Figure 1 Growth curves and adiposity of TNF-$\alpha^{-/-}$ and TNF-$\alpha^{+/+}$ mice. **a**, Development of diet-induced obesity in TNF-$\alpha^{-/-}$ and TNF-$\alpha^{+/+}$ mice (n = 10 in each group). **b**, Epididymal fat-pad weights of TNF-$\alpha^{-/-}$ and TNF-$\alpha^{+/+}$ mice.

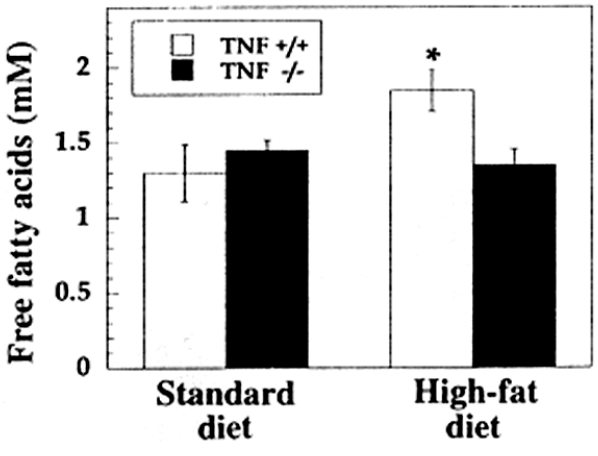

Figure 4 Circulating free fatty-acid levels in TNF-$\alpha^{-/-}$ and TNF-$\alpha^{+/+}$ mice. Asterisk indicates $P < 0.05$; two-tailed Student's t-test comparing free fatty-acid levels in TNF-$\alpha^{-/-}$ and TNF-$\alpha^{+/+}$ mice.

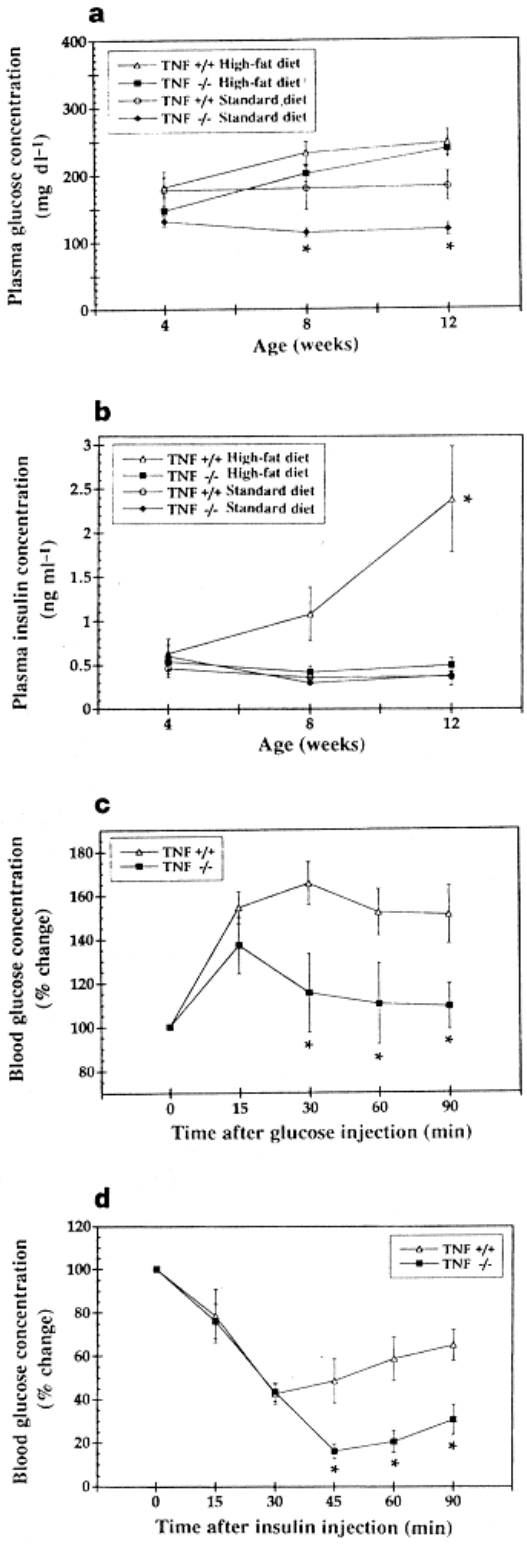

Figure 2 Measures of glucose homeostasis in TNF-$\alpha^{-/-}$ and TNF-$\alpha^{+/+}$ mice. **a**, **b**, Fasting glucose (**a**) and insulin (**b**) concentrations. **c**, **d**, Glucose (**c**) and insulin (**d**) tolerance tests. Asterisks indicate $P < 0.05$. Investigations of the dynamics of the responses to the tolerance tests were done by ANOVA repeated measures analysis (Statview 4.01, Abacus Concepts), and demonstrated statistically significant differences between the TNF-$\alpha^{-/-}$ and TNF-$\alpha^{+/+}$ mice in both tests ($P < 0.05$).

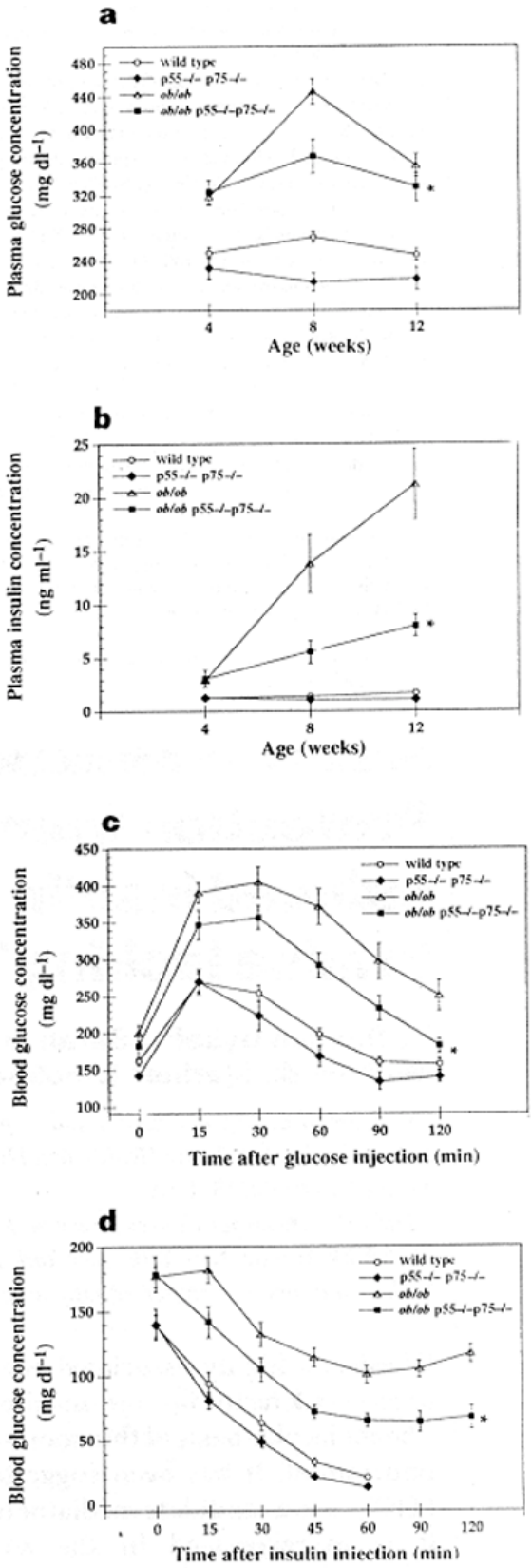

Figure 3 Measures of glucose homeostasis in *ob/ob* and *ob/ob* $p55^{-/-}p75^{-/-}$ mice. **a**, **b**, Fasting plasma glucose (**a**) and insulin (**b**) concentrations. **c**, **d**, Glucose (**c**) and insulin (**d**) tolerance tests. Mice studied: *ob/ob* ($n = 51$ in **a** and **b**, and 41 in **c** and **d**); *ob/ob* $p55^{-/-}p75^{-/-}$ ($n = 17$). Asterisks indicate $P < 0.05$.

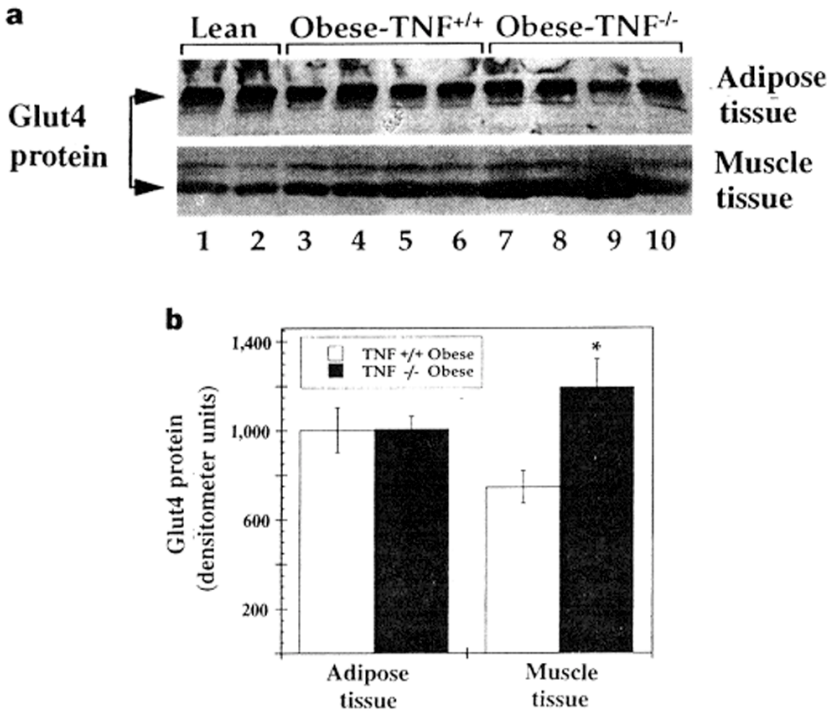

Figure 5 The levels of Glut4 protein in TNF-$\alpha^{-/-}$ and TNF-$\alpha^{+/+}$ mice. **a**, A representative immunoblot showing Glut4 protein level in fat and muscle tissues. **b**, Immunoblots are quantified by NIH Image 3.01 image-analysis software and presented as arbitrary units. Six mice were used in each analysis in two independent experiments. Asterisk indicates $P < 0.05$.

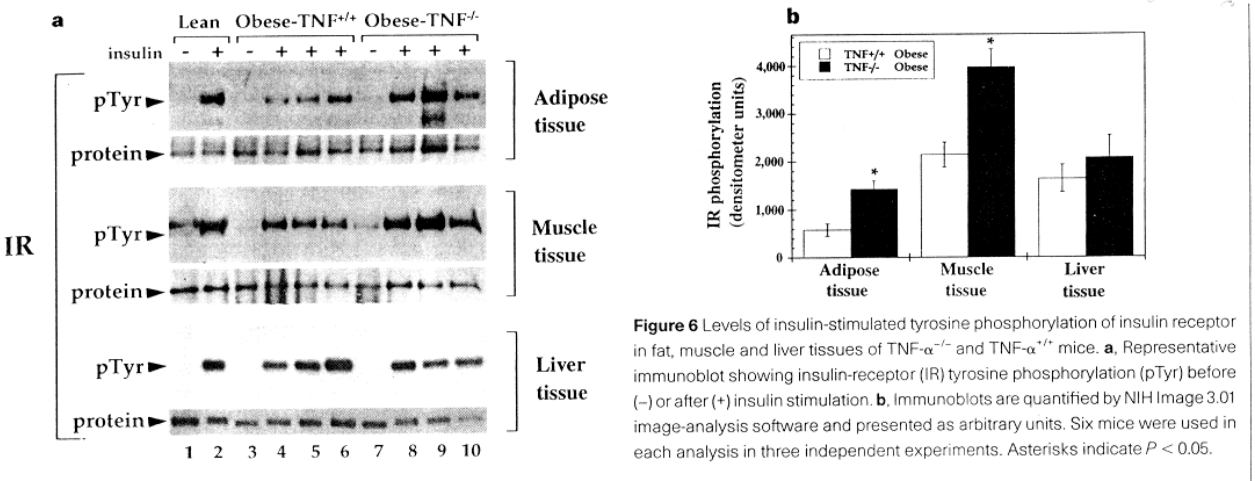

Figure 6 Levels of insulin-stimulated tyrosine phosphorylation of insulin receptor in fat, muscle and liver tissues of TNF-$\alpha^{-/-}$ and TNF-$\alpha^{+/+}$ mice. **a**, Representative immunoblot showing insulin-receptor (IR) tyrosine phosphorylation (pTyr) before (–) or after (+) insulin stimulation. **b**, Immunoblots are quantified by NIH Image 3.01 image-analysis software and presented as arbitrary units. Six mice were used in each analysis in three independent experiments. Asterisks indicate $P < 0.05$.